SAND79-0415
Unlimited Release

MASTER

ACCEPT: A Three-Dimensional Electron/ Photon Monte Carlo Transport Code Using Combinatorial Geometry

John A. Halbleib, Sr.

Sandia Laboratories

Unlimited Release
SAND79-0415

ACCEPT: A Three-Dimensional Electron/Photon Monte Carlo Transport Code Using Combinatorial Geometry*

J. A. Halbleib, Sr.
Theoretical Division 4231
Simulation Technology Department 4230

Sandia Laboratories**
Albuquerque, New Mexico 87185

ABSTRACT

The ACCEPT code provides experimenters and theorists with a method for the routine solution of coupled electron/photon transport through three-dimensional multimaterial geometries described by the combinatorial method. Emphasis is placed upon operational simplicity without sacrificing the rigor of the model. ACCEPT combines condensed-history electron Monte Carlo with conventional single-scattering photon Monte Carlo in order to describe the transport of all generations of particles from several MeV down to 1.0 and 10.0 keV for electrons and photons, respectively. The model is more accurate at the higher energies with a less rigorous description of the particle cascade at energies where the shell structure of the transport media becomes important. Flexibility of construction permits the user to tailor the model to specific applications and to extend the capabilities of the model to more sophisticated applications through relatively simple update procedures. The ACCEPT code is currently running on the CDC-7600 (6600) where the bulk of the cross-section data and the statistical variables are stored in Large Core Memory (Extended Core Storage).

*This work is supported by the U. S. Department of Energy under Contract No. DE-AC04-76DP00789.

**A U. S. DOE facility.

Contents

Contents (continued)

Illustrations

1. Introduction

Over the past few years, a series of user-oriented Monte Carlo codes,[1-4] hereafter referred to as the TIGER series, has been developed for describing the generation and transport of the electron/photon cascade in multimaterial configurations. The members of this series are distinguished from one another by the symmetry of the one-dimensional or two-dimensional material geometries. The cross sections and sampling procedures are essentially the same for all members. Also, much of the input data is the same, and the structure of the outputs is quite similar. Consequently, once some facility has been acquired in the use of any one of these codes, users can apply the others with little additional effort. This report documents the extension of this series to the development of the ACCEPT* code, a three-dimensional coupled electron/photon Monte Carlo transport code employing combinational geometry.[5,6]

Of course, the SANDYL code[7] is an excellent three-dimensional code that has been successfully applied to a variety of problems. However, there is no existing version of the SANDYL code that can be run on the latest scientific computers. Other disadvantages relative to previous codes of the TIGER series are

a) complexity of input data,

*This is a user-participation acronym standing for "_____ Combinational Coupled Electron/Photon Transport." The user is invited to fill in the blank with a modifier (starting with the letter "A") that best describes his experience using the code.

b) limited estimates of statistical uncertainties of output data,

c) approximations for random walk steps that are truncated at logical boundaries (e.g., for purposes of talleying energy and charge deposition) within a homogeneous medium,

d) lower resolution in the sampling of electron angular deflections and bremsstrahlung production, and

e) lack of facility for incorporating the effects of macroscopic electromagnetic fields.

Until recently the SANDYL code employed a more detailed description of atomic shell ionization and relaxation than was available in the TIGER series. However, an update package[8] is now available for incorporating this improved theory into any of the TIGER series codes. Some versions of the SANDYL code also include improved angular scattering cross sections for electrons at low energies.[9] This improvement is also available in the TIGER series via update. These latter two updates are extensive, requiring substantial increases in the primary and secondary memory requirements, and a significant increase in run time. Consequently, because the effects of these improvements have been found to be negligible for all except certain specialized applications involving relatively low-energy sources (where other portions of the transport theory also become suspect), these updates are not considered to be a part of standard versions of the TIGER series codes.

This discussion would not be complete without mention of the BETA code,[10] another model with full three-dimensional capability. By comparison with the TIGER series and SANDYL

codes, BETA has many novel features. In particular, it makes extensive use of sophisticated variance reduction procedures. However we think it fair to say that it is generally a much more difficult code to run and that it has not been subjected to the same degree of experimental and theoretical verification. We make this assesssment of the BETA code without first-hand experience with its application.

The most essential difference between the ACCEPT and SANDYL codes is the use of combinatorial geometry in the former as opposed to a system of paraxial quadratic surfaces and cartesian planes in the latter. The inherent limitation of the latter is clear, while the combinatorial scheme is limited only by the extent of the library of body types. Consequently, the combinatorial scheme is potentially more general. The price that one pays for this increased flexibility is one of run time; the restricted form of the quadratic surfaces available in the SANDYL code makes the particle tracking logic simpler (faster) than that of the ACCEPT code. On the other hand, this is at least partially offset by the dynamic tracking logic in the combinatorial scheme.[5,6] Finally, we find the combinatorial method of specifying input zones in terms of solid bodies to be simpler, more intuitive and less ambiguous than specification in terms of boundary surfaces.

Documentation of previous codes in the TIGER series gave priority to the binary forms of the programs. However, it is now quite clear that users prefer the FORTRAN programs in UPDATE format. This is a consequence of a conscious effort

on our part to minimize the standard card input by minimizing the number of options available through this input. Instead, our philosophy has been to provide the internal logic for a great variety of options which remain inactive with the standard card input alone, but which may be activated via simple updates. In this report we discuss only the update version of the ACCEPT code, and much more effort will be devoted to a description of the options available through update.

We have attempted to organize this report in a user-oriented format similar to that of References 1, 2 and 3. Section 2 is devoted to code operation--the minimum amount of information required for running the code. Recognizing their importance to users, Section 3 presents a catalogue of the more useful options available through update. The casual user may find Section 2 sufficient. The more sophosticated user will want to take advantage of the increased capability provided by Section 3. Users wishing to generate additional options beyond those of Section 3 or to make major modifications to the code should become more familiar with the structure of the code as discussed in Section 4. Finally, in Section 5 we discuss procedures employed to verify the accuracy of the code.

Comments and suggestions and/or consultations on any difficulties that may arise in the application of this code are welcomed.

2. Operation

2.1 Control Deck

The FORTRAN version of the ACCEPT code in update format is available on the local system as a permanent disk file. Figure 1 shows the control deck for running from this file on the local CDC-7600 computer. The Small Core Memory (SCM) and Large Core Memory (LCM) requirements are 141 000 and 245 000 octal words, respectively. The SCM and LCM requirements are determined by subprograms DATPAC and ACCEPTS, respectively (see Section 4). The program is also compatible with the local CDC-6600 system where Central Memory (CM) and Extender Core Storage (ECS) replace SCM and LCM, respectively.

2.2 Problem Geometry

With the ACCEPT code the user employs the combinatorial-geometry[5,6] method in order to describe the three-dimensional material configuration of the problem. This task is accomplished in three distinct steps:

a. Defining the location and orientation of each solid geometrical body required for specifying the input zones,

b. Specifying the input zones as combinations of these bodies, and

c. Specifying the material in each input zone.

A. Body Definition. Combinatorial geometry is predicated upon the existence of a library of geometrical body types from which the user may choose in order to describe his problem configuration. The information required to specify each body type in a three-dimensional cartesian system is as follows:

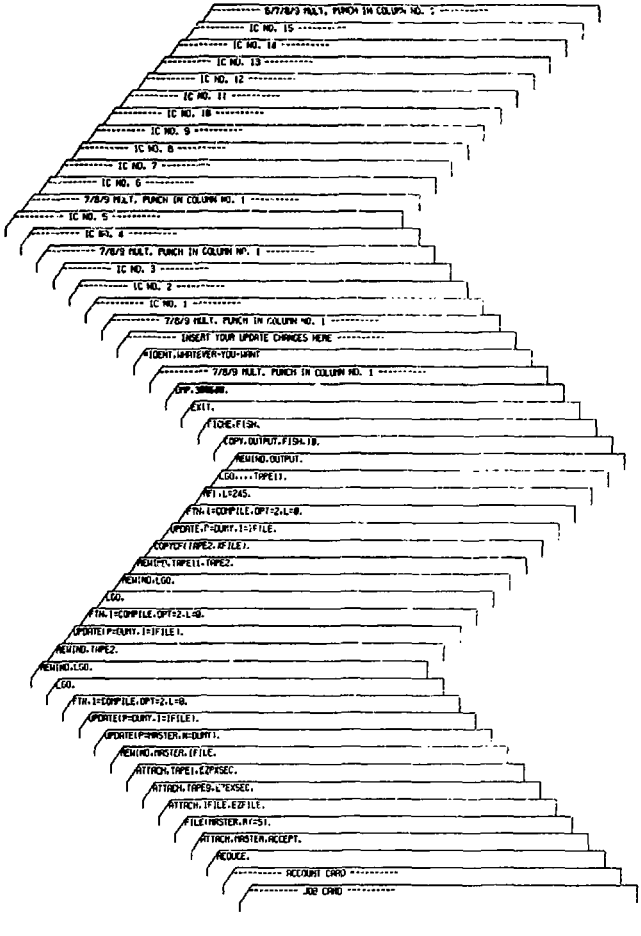

Figure 1. Control deck for running ACCEPT from permanent file.

a. Rectangular Parallelepiped (RPP)--Specify the minimum and maximum values of the x, y and z coordinates that bound a rectangular parallelepiped whose six sides are perpendicular to the coordinate axes.

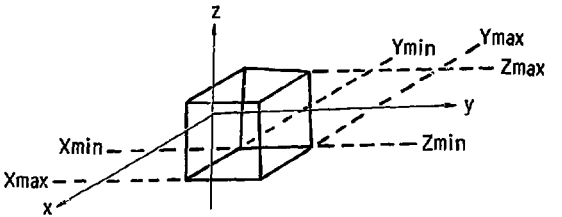

Figure 2. Rectangular Parallelepiped (RPP).

b. Sphere (SPH)--Specify the components of the radius vector, $\underline{V}$ to the center of the sphere and the radius, R, of the sphere.

Figure 3. Sphere (SPH).

c. Right Circular Cylinder (RCC)--Specify the components of a radius vector, $\underline{V}$, to the center of one base; the components of a vector, $\underline{H}$, from the center of that base to the center of the other base; and the radius, R, of the cylinder.

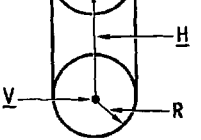

Figure 4. Right Circular Cylinder (RCC).

d. Right Elliptical Cylinder (REC)--Specify the components of a radius vector, $\underline{V}$, to the center of one of the elliptical bases; the components of a vector, $\underline{H}$, from the center of that base to the center of the other base; and the components of two vectors, $\underline{R_1}$ and $\underline{R_2}$, defining the major and minor axes, respectively, of the bases. This body has not yet been implemented.

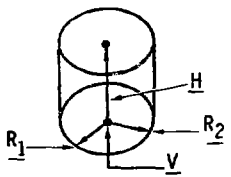

Figure 5. Right Elliptical Cylinder (REC).

e. Truncated Right Angle Cone (TRC)--Specify the components of a radius vector, $\underline{V}$, to the center of one base; the components of a vector, $\underline{H}$, from the center of that base to the center of the other base; and the radii, R_1 and R_2, of the first and second bases, respectively.

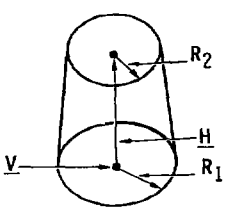

Figure 6. Truncated Right Angular Cone (TRC).

f. Ellipsoid (ELL)--Specify the components of the radius vectors, $\underline{V}_1$ and $\underline{V}_2$, to the foci of the prolate ellipsoid and the length of the major axis, R.

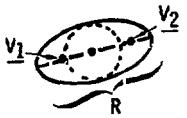

Figure 7. Ellipsoid (ELL).

g. Wedge (WED)--Specify the components of a radius vector, $\underline{V}$, to one of the corners and the components of three mutually perpendicular vectors, $\underline{a}_1$ and $\underline{a}_2$ and $\underline{a}_3$, starting at that corner and defining the wedge such that $\underline{a}_1$ and $\underline{a}_2$ are the two legs of the right triangle of the wedge.

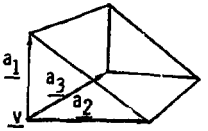

Figure 8. Right Angle Wedge (WED).

h. Box (BOX)--Specify the components of a radius vector, $\underline{V}$, to one of the corners and the components of three mutually perpendicular vectors, $\underline{a}_1$ and $\underline{a}_2$ and $\underline{a}_3$, starting at that corner and defining a rectangular parallelepiped of arbitrary orientation.

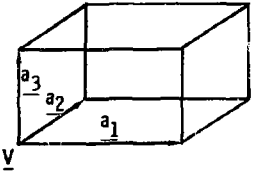

Figure 9. Box (BOX).

i. Arbitrary Polyhedron (ARB)--Specify the components of k (k = 6, 7 or 8) radius vectors, $\underline{V}_1$ through $\underline{V}_k$, to the corners of an arbitrary nonreentrant polyhedron of up to six sides; a final card contains a series of four-digit floating point numbers between "1230." and "8765." (enter zero for the fourth index of a three-cornered face), specifying the indices of the corners of each face. These indices must appear in either clockwise or counterclockwise order.

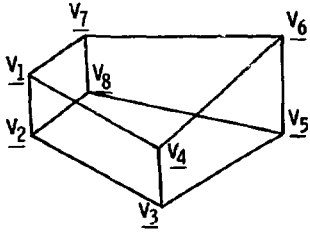

Figure 10. Arbitrary Polyhedron (ARB).

Detailed input instructions are given in Section 2.3.

B. Specification of Input Zones. Having defined the necessary geometrical bodies, the user must then resolve the entire problem geometry into input zones satisfying the following criteria:

a. An input zone may consist only of either a single homogeneous material or a void.

b. Every point of the problem geometry must lie within one and only one input zone.

c. The final input zone must be a void zone surrounding the rest of the problem geometry; any particle entering this zone is tallied as an escape particle.

Input zones are specified as appropriate combinations of the previously defined bodies. Such combinations may be as simple

as just a single body, or they may consist of complex intersections, unions and differences of various bodies. We illustrate the principles of input zone specification with the following examples where, for simplicity, we omit the escape zone. Each example involves only two zones, A and B, defined by the cross-hatching in Figure 11.

In Figure 11a, zone A consists of a sphere, body #1, that is tangent to zone B which consists of a right circular cylinder, body #2. Input zone specification is simply

$$A = +1$$

$$\text{and } B = +2 \ .$$

That is, input zone A consists of all spatial points that lie within body #1, and similarly for zone B.

In Figure 11b, the sphere is inserted into a hole that has been cut in the cylinder so that

$$A = +1$$

$$\text{and } B = +2 - 1.$$

Thus, input zone B consists of all spatial points that lie within body #2 AND not within body #1. Input zone B is specified as the difference between two bodies.

In Figure 11c, bodies #1 and #2 consist of the same homogeneous material (or void), but they are imbedded within a second right circular cylinder, body #3, of another material. The specification is

$$A = OR + 1 \quad OR \quad +2$$

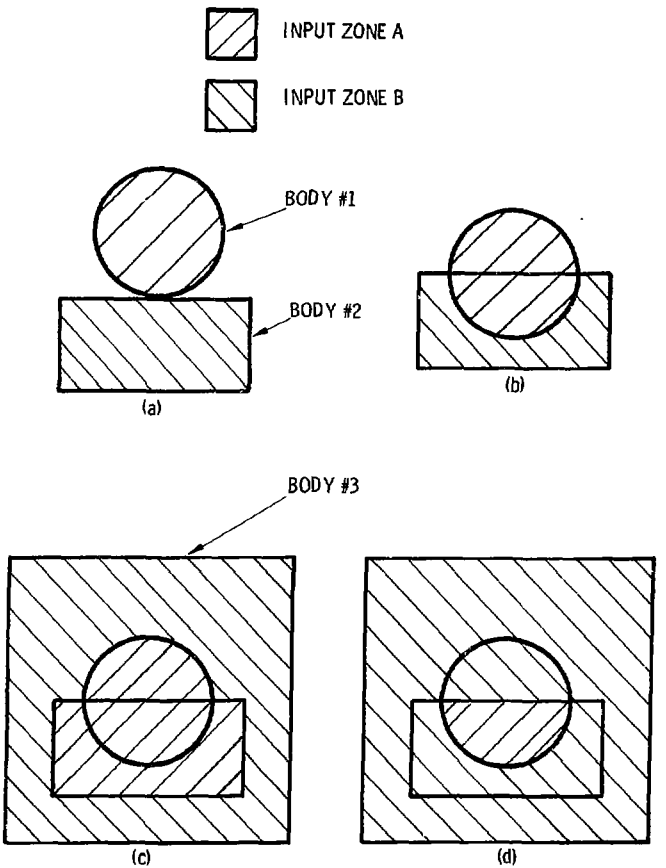

Figure 11. Illustration of various methods of combining bodies for specification of input zones.

and B = +3 - 1 - 2 .

Thus, input zone A consists of all spatial points that lie within EITHER body #1 OR body #2. This is an example of input zone specification as a union of bodies.

In Figure 11d, the intersection of body #1 and Body #2 consists of a single homogeneous material; the rest of the space within body #3 is filled with another material. The specification is

A = +1 +2

and B = OR +3 - 1 OR +3 - 2.

Thus, input zone A consists of all spatial points that lie within body #1 AND within body #2.

Note that

a. the OR operator refers to all following body numbers until the next OR operator is reached, and

b. the AND operator is implied before every body number that is not preceded by an explicit OR operator.

C. Material Specification. A material index is assigned to each input zone. A zero index identifies a void zone.

2.3 Input

Table I lists the card input variables required for each input card (IC) and the formats under which they are read. Note that, except for the combinatorial geometry data (IC's #7 through #10) and some of the more general source parameters

Table I: Input Variables and Formats

IC No.	Variables	Format
1	NMAT, NSET	(12I6)
2[a]	NE	(I5)
3[a]	(IZ(J), W(J), J=1, NE)	(5(I5,E10.0))[b]
4	COMMENT	(18A4)
5[a]	ISTATE, EMAX, RHO, ETA	(I5,3F12.5)
6	INC, JMAX, JPMAX, KMAX, KPMAX, IMAX	(12I6)
	*** COMBINATORIAL GEOMETRY DATA ***	
7	IVOPT, IDBG, (JTY(J), J=1, 15)	(2I5,10X,15A4)
8	ITYPE, (FPD(J), J=1, 6)	(2X,A3,5X,6E10.3)[b]
9	IALP, (IIBIAS(J), JTY(J), J=1, 13)	(2X,A3,13(A2,I3))[b]
10	(MAT(J), J=1, NZON)	(14I5)[b]
	*** SOURCE DATA ***	
11	XSR, YSR, ZSR, CTSR, CPSR, SPSR	(6F12.5)
12	TIN, TCUT, TPCUT, CTHIN, SORCIN	(6F12.5)
13[c]	JSPEC	(I6,66H)
14[c]	(SPECIN(J), J=1, JSPEC)	(6F12.5)[b]
15[c]	(ESP(J), J=1, JSPEC)	(6F12.5)[b]

[a]The pair of IC's, #2 and #3, and IC #5 are to be repeated NMAT times. The order of the repeated pair, #2 and #3, must correspond to that of the repeated IC #5.
[b]Use additional cards if necessary.
[c]Required only for nonmonoenergetic source (see Section 2.5).

(IC's #11 and #12, card input for the ACCEPT code is nearly identical with that of other codes of the TIGER series.

The variables listed in Table I are defined as follows:

NMAT: Number of unique materials, excluding voids, required in the problem: (≤ 5).

NSET: Arbitrary set number assigned by the user to be used for identification of the run.

(The two cards containing the next three variables must be repeated NMAT times. The order in which the pairs of the cards are read defines the material numbers required on IC #10.)

NE: Number of elements in the homogeneous target material: (≤ 10).

IZ: Array of atomic numbers of constituent elements read in ascending order.

W: Weight fraction array corresponding to the IZ-array.

COMMENT: A 72-character comment describing the run.

(The card containing the next four variables must be repeated NMAT times in the same order as the pairs IC #2 and IC #3.)

ISTATE: 1 for a solid or liquid; 2 for a gaseous target material.

EMAX: Incident energy (MeV) for monoenergetic source (electrons or photons) or maximum energy in the case of a source spectrum.

RHO: NTP (0°C, 1 atm) density of the target material (g/cm^3).

ETA: Ratio of actual density to the NTP density of the target material. If left blank (zero), ETA is automatically set to 1.0.

INC: 1 for incident electrons; 2 for incident photons.

JMAX: Number of equal energy bins for classifying escaping electrons ($\leq$ 50).

JPMAX: Number of equal energy bins for classifying escaping photons ($\leq$ 50).

KMAX: Number of equal angular bins for classifying the escaping electrons according to their obliquity with respect to the Z-axis ($\leq$ 36).

KPMAX: Number of equal angular bins for classifying the escaping photons according to their obliquity with respect to the Z-axis ($\leq$ 36).

IMAX: Number of histories of primary particles (electrons or photons) to be followed.

(The next four IC types are used to describe the problem configuration, using the combinatorial-geometry method as described in Section 2.2.)

IVOPT: Blank (zero) if zone volumes are to be internally set equal to 1.0, and 1 if they are to be read in immediately after the IC #9 cards under a 7E10.5 format (the order in which they are to be read is established by the sequence of the IC #9 cards).

IDBG: If not left blank (zero), results of combinatorial geometry calculations will be printed during execution. Use only for debugging as excessive print out may result.

JTY(IC#7): Alphanumeric title for geometry input.

ITYPE: Three-letter abbreviation of body type (as given in Section 2.2A) for initiating description of new body; blank for continuation cards when more than six FPD elements are required in the body description; and END in order to terminate the reading of body data. See Table II for examples.

FPD: Real data required for the given body as shown in Table II and defined in Section 2.2A. All lengths should be given in cm.

IALP: Any nonblank entry except END initiates description of a new input zone; a blank field indicates that this card is continuing the description of the input zone being described by the previous card; and END denotes the end of input zone description.

Table II: Body Data Required for IC #8

Body Type	ITYPE	Real Data Defining Particular Body						Number of Cards Needed
BOX	BØX	Vx	Vy	Vz	A1x	A1y	A1z	1 of 2
		A2x	A2y	A2z	A3x	A3y	A3z	2 of 2
Right Parallelepiped	RPP	Xmin	Xmax	Ymin	Ymax	Zmin	Zmax	1
Sphere	SPH	Vx	Vy	Vz	R	--	--	1
Right Circular Cylinder	RCC	Vx	Vy	Vz	Hx	Hy	Hz	1 of 2
		R	--	--	--	--	--	2 of 2
Right Elliptic Cylinder	REC	Vx	Vy	Vz	Hx	Hy	Hz	1 of 2
		R1x	R1y	R1z	R2x	R2y	R2z	2 of 2
Ellipsoid	ELL	V1x	V1y	V1z	V2x	V2y	V2z	1 of 2
		R	--	--	--	--	--	2 of 2
Truncated Right Cone	TRC	Vx	Vy	Vz	Hx	Hy	Hz	1 of 2
		R1	R2	--	--	--	--	2 of 2
Right Angle Wedge	WED	Vx	Vy	Vz	A1x	A1y	A1z	1 of 2
		A2x	A2y	A2z	A3x	A3y	A3z	2 of 2
Arbitrary Polyhedron	ARB	V1x	V1y	V1z	V2x	V2y	V2z	1 of 5
		V3x	V3y	V3z	V4x	V4y	V4z	2 of 5
		V5x	V5y	V5z	V6x	V6y	V6z	3 of 5
		V7x	V7y	V7z	V8x	V8y	V8z	4 of 5
		Face Descriptions (see note below)						5 of 5
Termination of Body Input Data	END							

Note: Card 5 of the arbitrary polyhedron input contains a four-digit real number for each of the faces. See Section 2.2A for more details.

Input zones are numbered sequentially from 1 through NZON as they are read in. The NZONth zone must be the escape zone as described in Section 2.2B.

IIBIAS: OR specifies the OR operator and a blank field implies the AND operator. See Section 2.2B.

JTY(IC#9): Body number with (+) or (-) sign as required for input zone description. See Section 2.2B. Body numbers are defined by the order in which the IC #8 cards are read in.

MAT: Array of numbers identifying the homogeneous material in each input zone. The number assigned to a nonvoid material is determined by the order in which the pairs, IC #2 and IC #3, are read in. Zero defines a void zone.

(The remaining IC types are used primarily to describe the standard source options. These options are shown schematically in Figure 12. The user may easily select other options via the update procedure described in Section 3.1.)

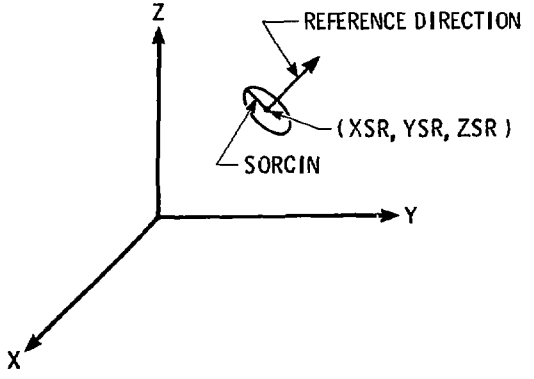

Figure 12. Illustration of standard source options.

XSR: X-coordinate of the source reference position.

YSR: Y-coordinate of the source reference position.

ZSR: Z-coordinate of the source reference position.

(This source reference position is internally shifted 10^{-7} cm along the reference direction defined by the next three input parameters in order to insure that all histories are initiated within some input zone other than the escape zone.)

CTSR: Cosine of the spherical polar angle of the source reference direction.

CPSR: Cosine of the spherical azimuth angle of the source reference direction.

SPSR: Sine of the spherical azimuth angle of the source reference direction.

TIN: Equals EMAX for monoenergetic source, minus EMAX for a nonmonoenergetic source.

TCUT: Cutoff energy (MeV) at which electron histories are terminated. A final adjustment pertaining to the calculation of energy and charge deposition is made ($\geq$ EMAX/244 or 0.001 MeV, whichever is the larger).

TPCUT: Cutoff energy (MeV) at which photon histories are terminated. Upon termination the residual energy of the photon is assumed to be deposited on the spot ($\geq$ 0.010 MeV).

CTHIN: Defines the angular distribution of source particles with respect to the source reference direction: blank (0.0) specifies a monodirectional source; > 0.0 specifies an isotropic angular distribution truncated at an angle, measured with respect to the source reference direction, having a cosine equal to CTHIN-2.0 (i.e., $1.0 \leq$ CTHIN ≤ 3.0 for a truncated isotropic source); and < 0.0 specifies a cosine law distribution truncated at an angle, again measured with respect to the source reference direction, having a cosine equal to -CTHIN-2.0 (i.e., $-1.0 \geq$ CTHIN ≥ -3.0 for a truncated cosine law source).

SORCIN: Equals 0.0 (blank) for a point source at the source reference position, or equals the radius of a uniformly distributed disk source oriented normally to the source reference direction and centered at the source reference position (e.g., CTHIN = 0.0

and SORCIN >0.0 defines a uniform monodirectional beam of source particles).

JSPEC:* One plus the number of energy bins in the spectrum (i.e., the number of energy values) of the incident radiation ($\leq$ 51).

SPECIN:* Cumulative probability distribution for the spectrum of incident radiation in descending order. SPECIN(1) must equal 1.0 and SPECIN(JSPEC) must equal 0.0.

ESP:* Energy list corresponding to SPECIN. ESP(JSPEC) $\geq$ TCUT (TPCUT in the case of a photon source).

2.4 Sample Input for Monoenergetic Source

Figure 13 shows the input data for a problem involving a monoenergetic source. A 0.05-cm radius beam of 1.0-MeV electrons is normally incident (Z-direction) upon the base of a configuration similar to that shown in Figure 11d. We have added body #4 in order to define the escape zone. The intersection of bodies #1 and #2 is gold. The surrounding medium is aluminum.

2.5 Sample Input for a Source Spectrum

Figure 14 shows the input data for the same problem as in Section 2.4, but with a spectrum of source electrons up to a maximum energy of 1.0 MeV. The only changes relative to Figure 13 are:

a. The problem title has been changed.

b. TIN has been changed from 1.0 to -1.0.

c. The additional cards describing the spectrum (IC #13, IC #14 and IC #15) have been added immediately after IC #12.

The source energies will be sampled from the spectrum shown in Figure 15. Note that only that portion of the spectrum

---

* JSPEC, SPECIN, and ESP are read in only when TIN is negative.

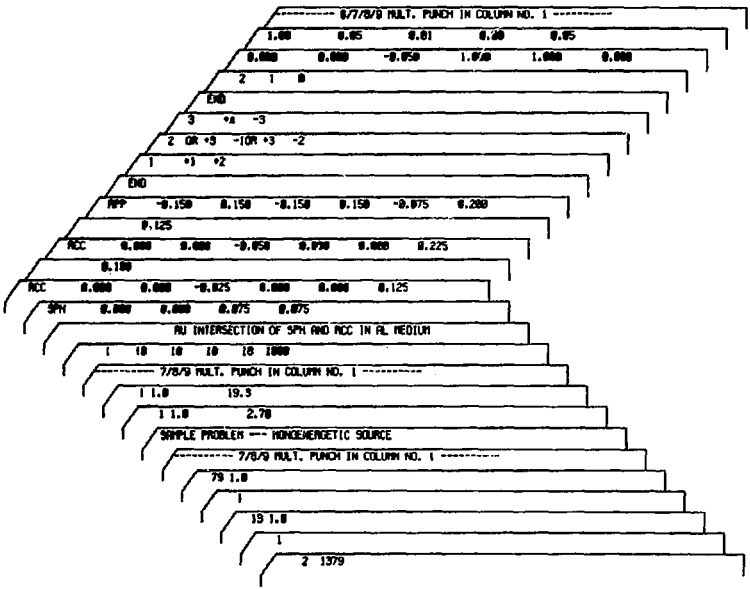

Figure 13. Sample input for running a problem with a monoenergetic source.

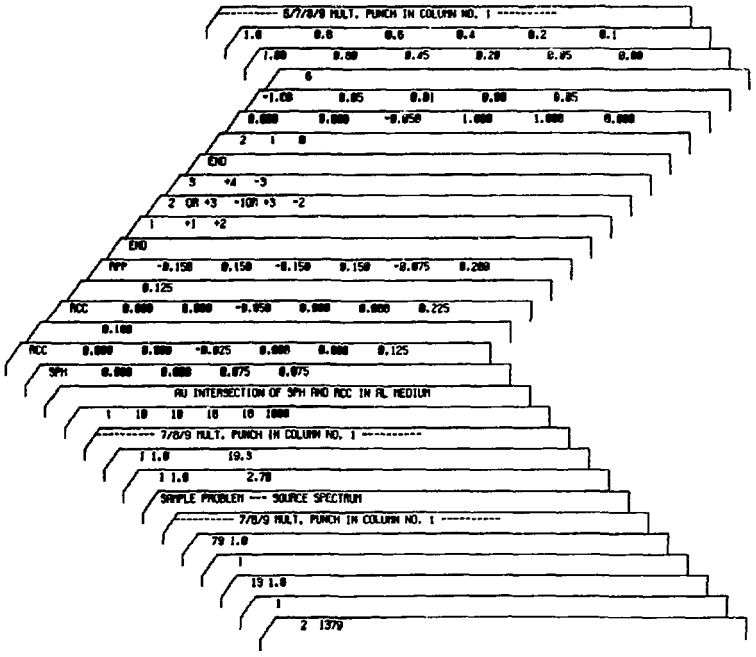

Figure 14. Sample input for running a problem with a nonmonoenergetic source.

above TCUT is employed in determining the cumulative distribution. For example, SPECIN(3), which is the fractional number of source electrons below 0.6 MeV but above TCUT (0.1 MeV), is given by

$$\text{SPECIN}(3) = \frac{5\% + 15\% + 25}{5\% + 15\% + 25\% + 35\% + 30\%} = 0.45 \ .$$

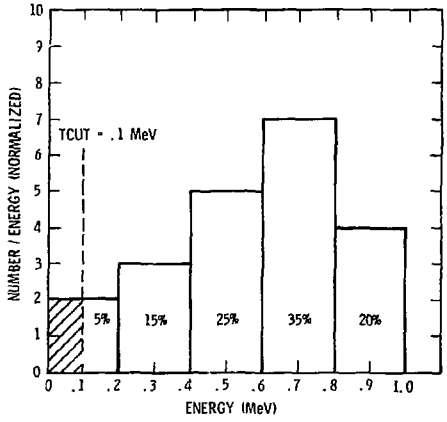

Figure 15. Source electron spectrum from which the cumulative probability distribution listed in Figure 14 was obtained.

2.6 Suggestions for Efficient Operation

Most of the operational limitations on input data are given in Section 2.3. However, because of the dynamic storage of the combinatorial geometry data, it is not possible to give a precise limit on the number of bodies and/or input zones. Body and zone data required in the Monte Carlo are close packed into a one-dimensional array which is currently dimensioned 3000 (decimal). If a user problem requires more than 3000 locations, the job will terminate with a diagnostic that this limit has been exceeded. The user must then use the update described in Section 3.10 to redimension this array. Finally, we wish to point out that the choice of certain input parameters can markedly affect the efficiency of the calculation; that is, the user's ability to obtain statistically meaningful output in a reasonable amount of time:

a. Obviously, the number of histories, IMAX, should be kept as small as possible. The ACCEPT code provides the user with estimates of the statistical accuracy of the output data.* This information serves as a guide in the choice of IMAX.

b. TCUT should be as large as possible. For example, if the source is monoenergetic, TCUT equal to 5 or 10 percent of TIN should be adequate. Because the logarithmic energy grid used in this technique becomes much finer at low energies, following histories down to low energies becomes very time consuming. On the other hand, running time is not very sensitive to the value of TPCUT.

c. JMAX, JPMAX, KMAX, KPMAX and the number of input zones should be as small as possible. Demanding excessive energy, angle, or spatial resolution

*See Sections 2.7 and 4.5F for further details.

only makes it more difficult to obtain statistically meaningful output.

2.7 Output

In addition to certain diagnostic information, the basic output consists of

a. Energy and number escape coefficients for electrons, unscattered photons and scattered photons.

b. Charge and energy deposition profiles.

c. Escape coefficients that are differential in energy for both electrons and scattered photons.

d. Escape coefficients that are differential in angle for both electrons and scattered photons.

e. Coupled energy and angular distributions of escaping electrons and scattered photons.

Every output quantity is followed by a one- or two-digit integer that is an estimate of the 1-sigma statistical uncertainty of that quantity expressed in percent. Details of the method used to obtain these statistical data are given in Section 4.5F.

3. Updates

In the development of the ACCEPT code our primary motivation was to provide scientists and engineers with a method characterized by both theoretical rigor and operational simplicity for routine solution of three-dimensional multimaterial problems. The rigor was achieved through the internal selection of the most general options. Operational simplicity is the keynote of Section 2. However, the analogue nature of the Monte Carlo procedure, the completeness with which the ACCEPT code describes the radiation transport, and the flexibility of construction

make it possible for the user to significantly extend the capabilities of the code with relatively simple updates. In this section several updates that the authors have found useful are reviewed in varying degrees of detail. The list is by no means exhaustive, and users are encouraged to consult with the authors concerning specific applications.

3.1 Source Routines

As the material geometries of transport codes become more complex, the possible types of source distributions become more numerous. We have chosen not to overwhelm the user with a myriad of choices. Instead, we have provided only those relatively basic choices described in Section 2.3. The resulting simplicity and flexibility in the coding of the source routine make it easy for the user to construct a source with arbitrary spatial, energy and angular distributions. To facilitate modification of source distributions, the relevant portions of subroutines INPUT and HIST of subprogram ACCEPTS are delineated by comment statements.

The only essential restriction on the source distributions is that any history must be initiated within some input zone other than the escape zone. In order to insure that this restriction is satisfied in the standard source routine, the source reference position (XSR, YSR, ZSR) is shifted 10^{-7} cm in the reference direction defined by the parameters CTSR, CPSR and SPSR.

3.2 Photon Path Length Stretching

Through update, the user may decrease (increase) the photon interaction probability relative to its natural value by updating the zone-dependent stretching (shortening) parameter, PTCZ(I), where I is the input zone index defined by the order of the IC-#9 cards. The photon cross section for the Ith input zone is scaled by the factor, 1/PTCZ(I). Without update PTCZ(I) is internally set equal to 1.0. In a manner identical to that employed for the ECUT parameter in Section 3.3, the user merely resets the values for those zones for which he wishes to make a change immediately after statement 411 in subroutine INPUT of subprogram ACCEPTS using the update instruction,

```
*INSERT,ACCEPT.29
```

followed by FORTRAN cards redefining the PTCZ parameter for the appropriate zones.

3.3 Zone-Dependent Electron Cutoff Energy

Through this update the user may increase the electron cutoff in any zone or zones above TCUT in a manner identical to that employed for the PTCZ parameter in Section 3.2. When, for example, the user wishes to raise the cutoff in input zones 2 through 7 of a given problem configuration from TCUT to 2.0 MeV, he need only insert the update

```
*INSERT,ACCEPT.29
    DO 25 I = 2,7
 25 ECUT(I) = 2.0
```

Electron transport can be terminated in any zone by simply choosing TCUT for the appropriate zone to be equal to the absolute value of TIN; the history will be terminated by the method used for electrons whose energies fall below TCUT. This update has also proved useful in problems which involve the generation of bremsstrahlung in one zone(s) and deposition due to that bremsstrahlung in another zone(s). A relatively high cutoff may be used in the converter zone(s), since low-energy electrons are relatively inefficient for producing bremsstrahlung. On the other hand, in the dosimeter zone(s) the user may be interested in the details of the deposition from the low-energy bremsstrahlung-produced secondaries or he may not want electron transport in those zones at all.

3.4 Trapped Electrons

In certain problems where only electrons that cross certain boundaries are important, the variable TSAVE may be employed through update to reduce running time significantly. Under normal operation TSAVE is internally set equal to TCUT, but it may be set equal to any value greater than TCUT through update. It becomes operational when an electron is trapped; that is, does not have enough energy to escape from a zone. When an electron with energy greater than TCUT but less than TSAVE is trapped, it is immediately terminated by the same method as for electrons whose energy falls below TCUT. This parameter is commonly used when one is primarily interested in those electrons escaping from all or some portion of the problem geometry. In this case the update is simply

```
*INSERT,EZTRN.295
      TSAVE = "desired value."
```

Great care should be taken in employing this update where bremsstrahlung production or effects may be important, since bremsstrahlung production is not allowed during terminal processing.

3.5 Scaling of Bremsstrahlung Production

This update is especially useful in bremsstrahlung converter studies. With the update

```
*INSERT,EZTRN.262
      BNUM(1) = "desired value,"
```

the user may artificially increase the bremsstrahlung production to improve the statistical accuracy of bremsstrahlung output without increasing the number of primary electron histories, which would be much more time consuming. The cross sections of material #1 are scaled so that an electron slowing-down from TIN to TCUT in this material will, on the average, generate BNUM(1) bremsstrahlung photons. The resulting scale factor is used to scale the bremsstrahlung cross sections for all other materials in the problem. Material #1 should be that material which one would expect to dominate the bremsstrahlung production. Simultaneous scaling of the K-shell impact ionization probability may be desirable (see Section 3.6).

This update is used primarily for the prediction of external bremsstrahlung production (e.g., prediction of the environment of x-ray sources). Consequently, a Russian Roulette procedure is employed to reduce the number of secondary electrons generated

from the interaction of this artificially high bremsstrahlung population to the naturally occurring number. Although this procedure is very efficient for predicting external bremsstrahlung, it leads to statistically poor and sometimes misleading results for bremsstrahlung deposition. In the latter case, the additional update

```
*INSERT, TIGER.225
  DLIM(L) = 1.0
```

will ensure that all secondary electrons are followed.

3.6 Scaling the Probability for K-Shell Impact Ionization

An update option similar to that of the previous subsection permits the user to artificially increase characteristic x-ray production by scaling the cross section for electron impact ionization of the K-shell of the highest-atomic-number element in each material. With the update

```
*INSERT,EZTRN.262
     XNUM =  "desired value,"
```

the K-ionization cross section of each material is scaled so that an electron slowing-down in that material from TIN to TCUT will, on the average, generate XNUM K-ionization events.

3.7 Substep Size

DRANGE/ISUB (see DATPAC output) is the substep size in g/cm^2. When not updated, ISUB is generated internally as a function of material atomic number. In certain applications, the substep size may be comparable to the dimensions of some input zones. This can lead to inaccuracies in condensed-history[11]

Monte Carlo. It is suggested that the chosen value of ISUB be sufficiently large that the maximum value of DRANGE/ISUB is no larger than one-tenth of the minimum dimension of any zone. The update is

```
*INSERT,EZTRN.80
   IF (NRUN .EQ. "desired value") ISUB = "desired value,"
```

where NRUN is the material index as defined by the order in which the pairs, IC#2 and IC#3, are read.

3.8 To Calculate Volumes of Input Zones

The user who wishes to insert his own logic for calculating the volumes of input zones need only set IVOPT equal to 2 on IC#7 and modify subroutine GENI of subprogram ACCEPTS using the update instruction,

```
*DELETE,ACCEPT.460,ACCEPT.462
```

followed by the FORTRAN logic for the volume calculation. These volumes are to be stored in the VNOR array. This array is available to the user in the edit routine, subroutine OUTPUT, where it may be employed to normalize selected output tallies via additional updates.

3.9 Multiple Problems

The user may obtain the results for an arbitrary number of problems in a single run with the update

```
*DELETE,ACCEPT.21
     IPNMAX = "desired value."
```

IC's #1 through #5 are not repeated; they must contain sufficient information for the production of all electron and photon cross

sections required for the multiple Monte Carlo calculations. The group of IC's beginning with #6 must be repeated for each problem. This update is especially useful in parameter studies. Although its use will prevent multiple turnaround time and repetition of cross-section calculations, it must be remembered that a multiple problem run necessarily requires more machine time.

3.10 To Extend the Length of the Body/Input-Zone Array

Normally, the single-variable common block labeled COG is dimensioned for 3000 decimal locations of SCM. To either increase or decrease this number, depending upon the geometrical complexity, the user must do the following:

(a) Redimension to the appropriate value the single-variable in common block COG within the several subroutines of subprogram ACCEPTS in which this common block appears.

(b) Insert the update

```
*DELETE,ACCEPT.152
     DATA KDMAX/"desired value"/
```

3.11 To Change the Number of Allowed Input Zones

To change the number of allowed input zones, the user simply redimensions the appropriate variables in common blocks OUT and PUNK of subroutine OUTPUT of the ACCEPTS subprogram. The appropriate variables in common block OUT have been grouped together to facilitate this update.

3.12 To Extend the Length of the Statistical Arrays

Normally, the two statistical arrays, ECAVE and ECSIG, are each dimensioned for 5000 decimal locations of LCM. To either increase or decrease this number, depending on the amount of output from the run, the user must do the following:

(a) Redimension ECAVE and ECSIG to the appropriate value in subroutine STATS of subprogram ACCEPTS.

(b) Insert the update

```
*DELETE,C2/20/79.12
     KPTMAX = "desired value."
```

(c) Correspondingly increase or decrease the total LCM request.

3.13 To Increase the Allowed Number of Homogeneous Materials

Without update the ACCEPT code is dimensioned for problems involving up to five homogeneous materials. The following steps may be employed to redimension for an arbitrary number of materials so long as the available SCM and LCM are not exceeded:

(a) Redimension all variables in common blocks OUT, CALC and XPED having a dimension of 5 (five) to the desired number of materials. This need only be done in one routine (e.g., subroutine INPUT of subprogram ACCEPTS) since these common blocks are parts of common decks.

(b) Scale the dimensions of the variables, ECHANG, ECBDIS, ECG, ECSURV and ECPAIR by the ratio of the desired number of materials to 5 (five). Again, this need only be done in one routine of subprogram ACCEPTS as it is also part of a common deck.

(c) Redimension all variables in common block TEMP of subroutines XINPUT, XPREP and PTAB (i.e., three places) of subprogram ACCEPTS having a dimension of 5 (five) to the desired number of materials.

(d) In subprogram PGEN, redimension variables IZ, W, ZZ, AZ and NE for the desired number of materials instead of 5 (five).

3.14 Pulse Height Distribution (PHD)

In order to obtain a PHD (or, more correctly, a spectrum of absorbed energy) for his problem, the user must do the following:

(a) He must insert the update

```
*DELETE,PHD.4
    IPHD = 1
```

(b) Immediately after the card input data listed in Table I (see subroutine INPUT of subprogram ACCEPTS), he must provide the variables JSMAX, LSB and LSE under a 12I6 format. JSMAX ($\leq$ 50) is the number of energy channels for the PHD. The PHD will be calculated for that portion, and only that portion, of the problem which is described by input zones LSB through LSE. Thus the active zones must be numbered sequentially from LSB through LSD, when setting up the input zone cards, IC #9 in Table I.

(c) Immediately after the input card described in (b), the user must supply the energy channels in MeV under a 6F12.5 format.

Important Note: No biasing of any kind is permitted when this option is activated. For example, the updates described in Sections 3.2, 3.5 and 3.6 are not to be used when a PHD is being calculated.

3.15 Spatial and Energy Distributions of Electron and Photon Fluxes

The user may obtain volume-averaged (track-length) spatial and energy distributions of internal electron and/or gamma fluxes as follows:

(a) Insert the update

```
*DELETE,ACCEPT.48
    IFLUX = 2 (electron flux only)
            3 (photon flux only)
            4 (both electron and photon
              flux)
```

(b) If IFLUX equals 2 or 4, read IFMK, JFMAX, LFB and LFE under a 12I6 format immediately after IC #15 where

IFMK selects the method of defining lower bounds of energy bins (see subroutines INPUT and ELIST of subprogram ACCEPTS),

JPMAX defines the number of energy bins,

LFB defines the first zone of an arbitrary sequence of input zones for which the electron flux is to be calculated, and

LFE defines the last zone of this arbitrary sequence of input zones for which the electron flux is to be calculated.

(c) If IFLUX = 3 or 4, photon data corresponding to (b) is read.

(d) Redimension flux variables in common blocks FLUX and PUNK of subroutine OUTPUT of subprogram ACCEPTS, where

FLUX, FMARK, FNUM, FCONT and FPRINT are the electron variables; and FLUXP, FMARKP, FCONTP and FPRNTP are the photon variables.

3.16 Azimuthal Dependence of Escape Coefficients

It is possible for the user to obtain azimuthal dependence of escape coefficients, assuming symmetry about an azimuth angle of zero. Without update, the ACCEPTS subprogram is dimensioned for a single azimuth bin. To increase the number of azimuth angles, the user must do the following:

(a) Update the FORTRAN statements in subroutine INPUT defining the variables KMAZ and KPMAZ, which are the number of azimuthal bins for electrons and photons, respectively.

(b) Correspondingly redimension those arrays which contain azimuthal dependence. All such arrays may be found in subroutine OUTPUT. The array names are AZMARK, BZMARK, ZMARK, ZPMARK, ENANG1, PNANG1, EDIFF1, PDIFF1, CZCONT, BZCONT, AZPRT, BZPRT and PAINT1. In every case the last dimension is the azimuthal dimension.

If while making the changes described in item (b) the user also reduces the polar-angle and energy dimensions to those required for his problem, he will minimize or avoid any increase in the SCM requirement.

3.17 Photon Transport Down to 1.0 keV

Under this option, conventional single scattering photon Monte Carlo is extended down to 1.0 keV. Although edge effects are included in the photon cross sections, the effect of atomic ionization as well as fluorescence and Auger emission are still included only for the K-shell of the highest-atomic-numbered element of a given material. Due to the substantial increase in SCM and LCM required for this option, the 10.0 keV (or greater) cutoff remains standard. In order to obtain the 1.0-keV version the user must:

(a) Insert the update
*YANK,TENKEV

(b) Increase the LCM request for subprogram ACCEPTS to 415 000 (octal).

As discussed in Section 1, the more sophisticated model employed in the TIGERP code[8] could easily be adapted to the ACCEPT code.

3.18 Modified Scoring of Particle Escape

Without update all electrons and/or photons entering the escape zone are scored in the various escape tallies. The user may wish to restrict this scoring (for example, to just those escaping through a certain surface) or to spatially resolve escaping particles. This can be accomplished within the escape routines ESCORE (electrons) and PSCORE (photons). However, this may preclude verification of energy conservation since the integral escape coefficients are used for this verification.

3.19 To Change the Starting Random Number

The user may wish to select his own starting number. For example, he may wish to initiate a new run starting with the

final random number (labeled IRC in listed output) of the completed run. This is accomplished with the following update:

```
*DELETE,CORR19.1
     INRAN = "sixteen digit octal number followed by B"
```

3.20 To Print the Output from Every Batch

Normally, only the final batch is printed. To print every batch, the user employs the following update:

```
*DELETE,BUFFERS.17
     N = 6
```

4. Construction

Insofar as electron transport is concerned, the ACCEPT code, like other codes of the TIGER series, the SANDYL code and other less well-known codes, should be thought of as belonging to the same generic class of ETRAN-like codes. For, although there have been major improvements, modifications and extensions, most of the electron cross sections and many of the associated Monte Carlo algorithms originally developed for the ETRAN Monte Carlo code system[11,12] are still being used.

The ACCEPT code consists of two BCD permanent files, EZPXSEC and EZEXSEC, and a disk file named ACCEPT in update format which contains three subprograms. The two BCD files and the first two subprograms, which are used for cross-section generation, are also components of other codes of the TIGER series.

4.1 EZPXSEC

EZPXSEC, the photon-cross-section library, is essentially the cross-section data of Biggs and Lighthill[13,14] in modified

format and is identical with the photon library used in other codes of the TIGER series.

4.2 EZEXSEC

EZEXSEC, the electron-cross-section library, was constructed by Berger and Seltzer and is referred to in their ETRAN Monte Carlo code system[12] as LIBRARY TAPE 2. It is distinguished from other library tapes of the ETRAN system in that the empirical corrections to the bremsstrahlung cross sections are based upon the experimental data of Rester[15] and Aiginger.[16] This same cross-section library is employed in other codes of the TIGER series.

4.3 PGEN

PGEN is the first of three subprograms in update format which make up the ACCEPT file. Using the file EZPXSEC and the data from IC #1, IC #2 and IC #3 of Table I, it prepares the photon sampling distributions required by the Monte Carlo subprogram. These distributions cover an energy range from 1000 MeV down to 10 keV. This subprogram is identical with the corresponding subprogram of other codes of the TIGER series. It uses the data of Wapstra[17] for the average K-fluorescence energies. Again, fluorescence and Auger production are allowed for only the highest-Z element of each material, regardless of its weight fraction.

4.4 DATPAC

This second subprogram of the ACCEPT file prepares the electron sampling distributions for the Monte Carlo subprogram.

Using the EZEXSEC file, IC #5, and material data transferred from subprogram PGEN, it generates the same distributions as does the identical subprogram of other codes of the TIGER series.

4.5 ACCEPTS

ACCEPTS is the last of the three subprograms that make up the ACCEPT file. The construction of ACCEPTS constituted most of the effort in the development of the ACCEPT code. The Monte Carlo subprogram of the CYLTRAN code, while restricted to two-dimensional material geometries having cylindrical symmetry, already employs a full three-dimensional description of particle trajectories. It was this feature that made it especially suitable as the basis of a model for combining collisonal and macroscopic field transport.[4] For this same reason, it was chosen as the starting point in the development of the ACCEPT code. Also available was a local version of the MORSE[6] coupled neutron/gamma transport code which employed a combinatorial geometry scheme originally developed by Mathematical Applications Group, Inc. under contract to the Department of the Army.[5] In essence the ACCEPTS subprogram was obtained by replacing the geometrical structure of the Monte Carlo subprogram of the CYLTRAN code by a suitably modified version of the combinatorial scheme employed in the MORSE code, with additional requirements for adapting this scheme to the peculiar characteristics of condensed-history electron Monte Carlo.[11]

In the following subsections, we discuss the more important features of the ACCEPTS subprogram.

A. Trajectories. ACCEPT employs a full three-dimensional description of particle trajectories; particle position is specified in cartesian coordinates, and particle direction is described by the appropriate spherical polar angles.

The generation and transport of the electron/photon cascade within the problem configuration is accomplished to a degree of sophistication which is equivalent to that of Reference 12. Particle histories are followed until either they escape or their energies fall below the chosen cutoffs. In the latter case the residual photon energy is deposited on the spot, whereas a more elaborate terminal approximation procedure--a generalization to three dimensions of the method employed in the TIGER code (see Section 4.5B of Reference 1)--is employed for the deposition of the residual energy and charge of electrons.

B. Boundary Crossings. Photon transport in the ACCEPT code is accomplished via conventional microscopic Monte Carlo methods[18] where particle trajectories which cross material boundaries pose no unusual problems. On the other hand, when the condensed-history Monte Carlo substep of an electron crosses a material boundary, certain approximations must be invoked. The procedures employed in the ACCEPT code are equivalent to those used in the TIGER code and are discussed in Section 4.5B of Reference 1.

There is one feature of the boundary-crossing logic of the ACCEPT code which represents an improvement over that employed in the present version of the SANDYL code.[7] The

logic of the SANDYL code is such that the approximations which must be invoked at material boundaries are called upon at all zone boundaries, even those which are not material boundaries. Thus, when a material is finely zoned for a high-resolution deposition profile, the inaccuracies of the boundary-crossing approximations are compounded many times. This effect has been observed in comparisons of one-dimensional profiles obtained from SANDYL with those obtained from the TIGER code where the problem does not arise. The problem can be avoided in SANDYL, and future versions will probably reflect this improvement. Because this problem was recognized in SANDYL beforehand, the logic of the ACCEPT code was constructed to distinguish between those boundaries that are material boundaries and those that are not. In the latter case the boundary-crossing approximations required for material boundaries are avoided.

C. Combinatorial-Geometry Routines. In Section 2.2, we gave a detailed discussion of the method of specifying the problem geometry. Here we give a brief description of those combinatorial-geometry routines which are required to process the body and input-zone data and to track the electron/photon cascade through the specified configuration. Where possible, we reference these routines to their counterparts in the CYLTRAN and MORSE codes.

a. Subroutine JOMIN is a modified combination of subroutines JOMIN1 and JOMIN2 of the local version of the MORSE code. JOMIN reads IC's #7, #8 and #9; writes the necessary body and

input zone data to an internal unit for subsequent access by subroutine GENI; determines the starting addresses of the various types of data to be stored in the body/input-zone array; and calls subroutine GENI.

b. Subroutine GENI is a modified combination of subroutines GENI, ALBERT and GTVLIN of the local version of the MORSE code. GENI reads the body and input zone data provided by JOMIN; close packs the body/input-zone array with the data required in the Monte Carlo calculation; executes the option selected for specifying the volumes of the input zones; and prints the combinatorial geometry specification of the problem configuration.

c. Subroutine ZONEA is a modified version of subroutine LOOK2 of the local version of the MORSE code, which generalizes the functions of subroutines ZONE and DIST of the CYLTRAN code to combinatorial geometry. Through calls to subroutine GG, ZONEA determines the input zone corresponding to the sampled source position; determines the uncollided distance to escape from this input zone using the sampled source position and direction; and dynamically stores source zone information in order to more efficiently determine the source zones of subsequent primary particles. Much of the coding in ZONEA is the same as that in the second half of subroutine DISTA.

d. Subroutine PR is a modified version of subroutine PR of the local version of the MORSE code. When the IDBG parameter on IC #7 is nonblank, PR is called by subroutines ZONEA, GG and DISTA. It prints the combinatorial tracking logic for debugging purposes.

e. Subroutine GG is an essentially unmodified version of subroutine GG of the local version of the MORSE code. It is also a generalization of subroutine DIST of the CYLTRAN code to combinatorial geometry. For a given particle position and direction, and a given body as defined by IC #8, GG employs the appropriate vector-analytic geometry to determine the uncollided distance to enter the body, uncollided distance to exit the body, surface of entry and surface of exit. The logic includes a check on the possibility that these data have already

been determined on a previous call, in which case they are retrieved from storage and control is returned to the calling routine (either ZONEA, DISTA or ANGLE).

f. Subroutine DISTA is a modified version of subroutine G1 of the local version of the MORSE code. It includes the combined functions of subroutines DIST and ZONE of the CYLTRAN code generalized to combinatorial geometry. DISTA is the primary tracking routine of the ACCEPT code. For a particle at a given position with a given direction in a given input zone, DISTA calculates the distance to escape from this zone and compares this distance with either the sampled interaction distance in the case of a photon or the condensed-history substep in the case of an electron. If the distance to escape is greater, control is returned to the calling routine (either EHIST or PHIST). Otherwise DISTA determines the new input zone encountered upon escape from the given input zone. The utility routine, GG, described above is an essential element of this tracking procedure. A very important feature of the method is its dynamic character, according to which the number of a zone being entered upon exit from the given zone is stored in order to improve the efficiency of the search upon subsequent exits from the given zone. It is also important to note that this dynamic storage can result in a substantial reduction of card input relative to that required in a code like SANDYL where this information must be supplied by the user. In deriving DISTA from G1, it was generalized so as to apply to both condensed-history electron transport (ICALL = 1) and single scattering photon transport (ICALL = 0). A special feature of the former derives from the a posteriori sampling of secondary production along the condensed-history substep of an electron. Specifically, it is necessary to apportion a substep which lies within more than one input zone of the same material in order to permit subsequent sampling of secondary events at random positions along that substep. Finally, the scheme for fractional forcing of photon interactions employed in the CYLTRAN code (see Section 5.7 of Reference 2) was not compatible with the logic of DISTA; consequently, this scheme was replaced by the path-length stretching procedure described in Section 3.2. Also, since escape of scattered photons is generally not so important in three-dimensional applications, the next-event estimator for photon

escape, which was very time consuming when used with combinatorial geometry, was eliminated.

g. Subroutine ZONE uses the data describing the apportionment of an electron condensed-history substep among more than one input zone of the same material, as determined in subroutine DISTA (see above), in order to determine the input zone in which a randomly sampled secondary event occurs.

h. Subroutine ANGLE is a generalization of subroutine ANGLE of the CYLTRAN code to combinatorial geometry. When a condensed-history substep is truncated at a material boundary, ANGLE uses geometry data from the most recent call to DISTA from EHIST in order to sample from the truncated multiple scattering distribution.

i. Subroutine ZONEC has no counterpart in the MORSE code since, like subroutines ZONE and ANGLE, it deals specificatlly with electron transport. It is a generalization to combinatorial geometry of the variance-reduction option in CYLTRAN for trapped electrons (see Section 3.4). As will be seen in Section 5, this option can significantly affect run times for certain problems. The derivation and coding of the method of determining the minimum distance to the surface of each of the nine body types, for both the (+) and (-) operators, constituted a significant fraction of the total effort required in the development of the ACCEPT code. Moreover, because of the complexity of the coding, extensive debugging and verification was required (see Section 5). For an electron having an energy between TSAVE (see Section 3.4) and TCUT, and located in a given code zone* consisting of an arbitrary combination of body types, subroutine ZONEC determines the minimum distance to the surface of that code zone* and compares this distance with the residual continuous-slowing-down-approximation range of the electron.

---

*Internally, the combinatorial logic is based more directly upon a set of code zones rather than the set of input zones defined by the IC #9 cards. If the OR operator is not used, the two sets are identical. The OR operator is used to define an input zone as the union of certain subzones. In the combinatorial logic these subzones are referred to as code zones. For example, the ACCEPT code internally breaks down input zone B of Fig. 11d into the two code zones, +3-1 and +3-2.

D. Void Zones. The additional logic required to accommodate void zones is considerable. This additional logic is avoided in some codes[7] by simulating voids with very low density gases. We believe allowance for actual voids to be preferable for three reasons. First, a faster code should result because void transport bypasses many collisional algorithms. Second, a more accurate code should result because void transport is rigorous, whereas condensed-history electron transport through small-areal-density simulated voids involves a number of approximations. Finally, a substantial amount of additional memory is required for the cross-section data of the simulation gas (see Section 4.5G).

E. Shell Effects. The treatment of ionization and relaxation effects within stopping media is not nearly so detailed in the ACCEPT code as it is in SANDYL. Photoionization and electron-impact ionization, as well as subsequent relaxation via fluorescent and Auger processes, are considered only in the case of the K-shell of the highest-atomic-number element of a given material. Photon transport below 10 keV is not allowed. Thus, for those applications in which shell ionization and relaxation effects are expected to have a significant effect upon the output of interest, the SANDYL code is to be preferred over the ACCEPT code. However, since it is independent of geometry, the update package described in Reference 8 could easily be adapted to the ACCEPT code.

F. Statistics. Under the normal default option, the IMAX histories are run in 10 equal batches. The output routine is

called at the end of each batch. Immediately before each write statement, a call is made to subroutine STATS. This routine recalls the statistical variables corresponding to the output quantities about to be written, computes the estimate of the standard error (in percent) based on the number of batches that have been run, and transfers the statistical parameters required for the subsequent batch back to LCM. Unless modified by update, only the final results based on the total number of completed batches are printed out. The user may specify a number of batches other than 10 by inserting the desired number in field 8 of IC #6.

A corollary of batch processing is a feature that prevents the user from exceeding his time limit. Before beginning a new batch, the remaining portion of the time requested for the job is compared with an estimate of the time per batch. If this estimate is larger than the time remaining, results based on the number of completed batches--including estimates of the statistical errors--are printed out and the run is terminated.

Under normal operation, virtually every Monte Carlo output quantity is followed by a one- or two-digit integer from 0 through 99 (estimates even greater than 99 are shown as 99) that is the best estimate of the statistical standard error expressed as a percent of the final value:

$$(S.E.)_N = \frac{100}{|\langle x_N \rangle|} \left(\left| \frac{\langle x_N^2 \rangle - \langle x_N \rangle^2}{N - 1} \right| \right)^{\frac{1}{2}} ,$$

where

$$\langle x_N \rangle = \frac{1}{N} \sum_{i=1}^{N} X_i \quad ,$$

and

$$\langle x_N^2 \rangle = \frac{1}{N} \sum_{i=1}^{N} x_i^2 \quad .$$

The X_i's are the values of the quantity obtained from each batch, and N is the total number of completed batches (usually 10).

G. Core Requirement. Core requirement was an important consideration in the construction of the ACCEPT code. About 15600 (decimal) variables are required for each material. Merely adding a material index to these variables would severely limit the number of materials allowed in a calculation. Furthermore, a large core requirement generally lowers job priority and increases turnaround time. The approach taken in SANDYL was to reduce the resolution of the larger distributions and to replace the largest, the bremsstrahlung energy and angular distribution, by a simple analytic formula. This approach was avoided in the construction of ACCEPTS by making use of LCM (ECS on the CDC-6600 system).

By putting the three largest electron-cross-section arrays in LCM and recalling them into SCM (CM on the CDC-6600 system) only when needed, the requirement for a material index for about 10000 of the above 15600 variables was avoided. Thus, only 10000 locations of SCM are required for these three arrays, regardless of the number of materials in the problem configuration. Two large photon-cross-section arrays, accounting for about 2700 of the 15600 variables, are also stored in LCM. These photon-cross-section variables are recalled individually, rather than by the entire array; thus, no central memory at all is required for these 2700 variables.* Since the remaining variables are arbitrarily dimensioned for five materials, the total LCM requirement for cross-section data is about 63500 (5 x 12700) decimal locations (see, however, the update in Section 3.13 for increasing the number of allowed materials).

An additional LCM requirement of 10000 decimal locations for statistical variables leads to a total LCM requirement of approximately 220000 octal locations (see, however, the update in Section 3.12 for increasing the size of the statistical arrays).

5. Verification

Ideally, code verification is best accomplished through direct comparison of code predictions with accurate experimental

*If this same procedure is used to eliminate the 27000 decimal locations required for the W1-array of the SANDYL code, about 65000 octal locations of Central Memory will be released. Furthermore, since the indexing arithmetic is already present in SANDYL, the increase in running time might be negligible.

data. This is not possible in the case of three-dimensional models because what little experimental data there is for complex geometries is even more suspect than the code results. However, accuracy of the modeling of the basic physical processes (i.e., cross sections and multiple interaction theories) can at least be inferred from comparisons of the predictions of simpler geometric models of the same generic class of ETRAN-like codes with high-quality experimental data. There have been many such comparisons[19] for various versions of the one-dimensional, single-material ETRAN code.[12] Further examples may be found in the documentation reports of the TIGER[20] and CYLTRAN[21] codes. Finally, during the last few years numerous results have been obtained from a combined experimental/theoretical program[22] directed specifically toward experimental verification of the TIGER code for electron sources at energies ≤ 1.0 MeV.

What we shall attempt to do in the remainder of this section is verify the overall numerical accuracy (coding) of the ACCEPT code through comparisons with other codes of the TIGER series, and through verification of internal consistency for geometrical configurations for which such comparisons are not possible. We shall do this by considering each of the eight active body types (the right elliptical cylinder has not yet been implemented) separately. Recognizing the importance of the variance reduction option for trapped electrons (see Section 3.4) which depends on the relatively complex analytic geometry

coding of subroutine ZONEC (see Section 4.5C), all comparisons will be repeated using the trapping update with TSAVE = TIN.

The logic for spheres and ellipsoids, with and without the trapping option, was verified through comparisons with predictions of the SPHERE code.[3] To test the logic for ellipsoids, we simply define the spherical bodies with degenerate ellipsoids--$\underline{V}_1 = \underline{V}_2$ in Section 2.2A. The geometry consists of a pair of nested Al spheres with a common center. The inner and outer spheres have radii of 5 cm and 9 cm, respectively. The two input zones are defined as the inner sphere and the region between the spheres so that both the (+) and (-) body logic will be tested. An isotropic source of 10.0 MeV (TIN) electrons is uniformly distributed over a third concentric spherical region having a radius of 6 cm. The source radius was chosen to thoroughly exercise the trapping logic when TSAVE = TIN. In each case 1000 histories were followed with a cutoff energy of 1.0 MeV (TCUT). Results are shown in Table III which compares the energy partition, charge deposition and run times. Agreement between the ACCEPT and SPHERE codes is very good. The fact that the ACCEPT/SPH and ACCEPT/ELL results are not identical when TSAVE = TIN is probably due to the use of a root finder for the ellipsoidal body in ZONEC, as opposed to the use of an analytic expression for the spherical body. It is also seen that use of the trapping option shifts a small amount of energy from deposition to escape since bremsstrahlung production is not allowed for trapped electrons. Unless one is specifically interested in the escape energy, the decrease in run time by

Table III: Comparison of predictions of the ACCEPT code with those of the SPHERE code. Numbers in parentheses are the estimated one-sigma statistical uncertainties expressed as percents of the given quantities.

		Energy Partition Fractions			Charge Deposition Fractions		
Code	TSAVE	Inner Zone Deposition	Outer Zone Deposition	Energy Escape	Inner Zone	Outer Zone	Run-Time (sec)
SPHERE	TCUT	.536(3)	.423(3)	.0445(6)	.548(3)	.452(4)	17.6
ACCEPT (SPH)	TCUT	.532(1)	.421(2)	.0474(5)	.543(2)	.452(2)	29.2
ACCEPT (ELL)	TCUT	"	"	"	"	"	31.3
SPHERE	TIN	.538(3)	.427(4)	.0364(5)	.517(4)	.481(4)	9.47
ACCEPT (SPH)	TIN	.534(2)	.430(3)	.0365(6)	.528(3)	.469(4)	16.3
ACCEPT (ELL)	TIN	.552(2)	.414(4)	.0342(9)	.551(4)	.448(5)	18.6

nearly a factor of two with the trapping option is probably more important than this small error. Furthermore, TSAVE = TIN yields the maximum possible trapping; because of the logarithmic energy grid employed in condensed-history electron transport and the strong energy dependence of bremsstrahlung production, a somewhat lower value of TSAVE would substantially improve the value for energy escape with relatively little increase in run time. Finally, it is clear that run time increases with either an increase in the complexity of the code or an increase in the complexity of the body type.

In analogous fashion the logic for right circular cylinders and truncated right angle cones, with and without the trapping option, was verified through comparisons with predictions of the CYLTRAN code.[2] To test the logic for truncated cones, we simply define the cylindrical bodies with degenerate truncated cones--$R_1 = R_2$ in Section 2.2A. The geometry consists of a pair of nested Al cylinders with a common center. The lengths of the cylinders are equal to their diameters. The inner and outer cylinders have diameters of 8 cm and 16 cm, respectively. The two input zones are defined as the inner cylinder and the region between cylinders. The 10.0-MeV isotropic source electrons are now distributed over a third concentric cylindrical region having both a diameter and length of 10 cm. Results are shown in Table IV. Agreement between the ACCEPT and CYLTRAN codes is very good. The above discussion of the results in Table III applies here also.

Table IV: Comparison of predictions of the ACCEPT code with those of the CYLTRAN code. Numbers in parentheses are the estimated one-sigma statistical uncertainties expressed as percents of the given quantities.

		Energy Partition Fractions			Charge Deposition Fractions		
Code	TSAVE	Inner Zone Deposition	Outer Zone Deposition	Energy Escape	Inner Zone	Outer Zone	Run-Time (sec)
CYLTRAN	TCUT	.481(3)	.480(3)	.0388(8)	.468(3)	.530(3)	19.2
ACCEPT (RCC)	TCUT	.460(3)	.489(3)	.0448(4)	.495(4)	.539(3)	35.1
ACCEPT (TRC)	TCUT	"	"	"	"	"	35.2
CYLTRAN	TIN	.472(2)	.491(3)	.0359(8)	.477(3)	.519(4)	11.9
ACCEPT (RCC)	TIN	.464(2)	.499(1)	.0392(10)	.448(2)	.551(1)	20.4
ACCEPT (TRC)	TIN	"	"	"	"	"	20.6

The logic for rectangular parallelepipeds, wedges, boxes and arbitrary polyhedrons, with and without the trapping option, has been verified through cross comparisons among results obtained from the ACCEPT code by using each of these bodies to describe the same physical problem. Each of these body types was used to describe a pair of nested Al cubes with a common center. The edges of the inner and outer cubes have lengths of 10 cm and 18 cm, respectively. The two input zones are defined as the inner cube and the region between the cubes. The 10.0-MeV isotropic electron source is now uniformly distributed over a third concentric cubical region having an edge length of 12 cm. Results are shown in Table V. Agreement among the four body types is very good. For a given choice of TSAVE, results are identical for all body types except the wedge. The wedge calculations required twice as many bodies as the others. Furthermore, in order to maximize logical testing, the ramps of the wedges defining the inner cube were perpendicular to the ramps of the wedges defining the outer cube. Consequently, the input zones were defined as unions* of intersections or differences of wedges. This unnecessarily complex zone description made the trapping option less effective (smaller reduction in run time) in the case of the wedge description. Even had all of the wedge ramps been parallel (coincident),

---

*Recall that unions increase the number of code zones over the number of input zones (see footnote in the discussion of subroutine ZONEC in Section 4.5C). Only those calculations in Table V using the wedge require unions in order to specify the input zones.

Table V: Comparison of predictions of the ACCEPT code for the same problem using different body types. Numbers in parentheses are the estimated one-sigma statistical uncertainties expressed as percents of the given quantities.

Body Type	TSAVE	Energy Partition Fractions			Charge Deposition Fractions		Run-Time (sec)
		Inner Zone Deposition	Outer Zone Deposition	Energy Escape	Inner Zone	Outer Zone	
RPP	TCUT	.539(3)	.422(3)	.0414(6)	.540(4)	.458(4)	32.8
BOX	TCUT	"	"	"	"	"	35.2
ARB	TCUT	"	"	"	"	"	48.2
WED	TCUT	"	"	.0491(6)	"	"	42.1
RPP	TIN	.549(3)	.420(4)	.0309(10)	.560(3)	.439(4)	16.9
BOX	TIN	"	"	"	"	"	18.4
ARB	TIN	"	"	"	"	"	24.6
WED	TIN	.553(2)	.416(3)	.0379(5)	.568(3)	.432(4)	28.2

when the trapping option was employed, the additional boundaries required in the wedge description alter the random number sequence relative to that of calculations using the other body types, leading to stochastically different results. On the other hand, the calculations without trapping were expected to yield identical results, independent of body type. Indeed the random number sequences were identical. However, the different escape energy in the case of the wedge calculation with TSAVE = TCUT is possibly due to slightly different numerical tolerances for different body types in subroutine GG. The above discussion of the results in Table III applies here also.

REFERENCES

1. J. A. Halbleib, Sr., and W. H. Vandevender, Nucl. Sci. Eng., 57, 94 (1975).

2. J. A. Halbleib, Sr., and W. H. Vandevender, Nucl. Sci. Eng., 61, 288 (1976).

3. J. A. Halbleib, Sr., Nucl. Sci. Eng., 66, 269 (1978).

4. J. A. Halbleib, Sr., and W. H. Vandevender, J. Appl. Phys., 48, 2312 (1977).

5. W. Guber, R. Nagel, R. Goldstein, P. S. Mettelman and M. H. Kalos, A Geometric Description Technique Suitable for Computer Analysis of Both the Nuclear and Conventional Vulnerability of Armored Military Vehicles, MAGI-6701, Mathematical Applications Group, Inc. (August 1967).

6. E. A. Straker, W. H. Scott, Jr. and N. R. Byrn, The MORSE Code with Combinatorial Geometry, SAI-72-511-LJ (DNA 2860T), Science Applications, Inc. (May 1972).

7. H. M. Colbert, SANDYL: A Computer Code for Calculating Combined Photon-Electron Transport in Complex Systems, SLL-74-0012, Sandia Laboratories (March 1973).

8. J. A. Halbleib, Sr., and J. E. Morel, Nucl. Sci. Eng., 70, 213 (1979).

9. L. G. Haggmark, C. J. MacCallum amd M. E. Riley, Trans. Am. Nucl. Soc., 19, 471 (1974).

10. T. M. Jordan, BETA-II, A Time-Dependent, Generalized Geometry Monte Carlo Program for Bremsstrahlung and Electron Transport Analysis, A.R.T.-60, A.R.T. Research Corporation (October 1971).

11. M. J. Berger, Monte Carlo Calculation of the Penetration and Diffusion of Fast Charged Particles, in Methods in Computational Physics, Vol. 1 (Academic, New York 1963).

12. M. J. Berger and S. M. Seltzer, ETRAN Monte Carlo Code System for Electron and Photon Transport Through Extended Media, CCC-107, Radiation Shielding Information Center, Computer Code Collection, Oak Ridge National Laboratory (June 1968).

13. F. Biggs and R. Lighthill, Analytical Approximations for X-Ray Cross Sections II, SC-RR-71 0507, Sandia Laboratories (December 1971).

14. F. Biggs and R. Lighthill, Analytical Approximations for Total Pair-Production Cross Sections, SC-RR-68-619, Sandia Laboratories (September 1968).

15. D. H. Rester and W. E. Dance, Electron Scattering and Bremsstrahlung Cross Sections, CR-759, National Aeronautics and Space Administration (April 1967).

16. H. Aiginger, Z. Fur Physik 197, 8 (1966).

17. A. H. Wapstra, G. J. Nijgh and R. Van Lieshout, Nuclear Spectroscopy Tables (International Publishers, Inc., New York, 1959) p. 81.

18. E. D. Cashwell and C. J. Everett, The Monte Carlo Method for Random Walk Problems (Pergamon Press, New York, 1959) p. 27 ff.

19. J. A. Halbleib, Sr., Electron Transport: Theory vs. Experiment, 100 keV to 10 MeV, unpublished survey (1971).

20. J. A. Halbleib, Sr., and W. H. Vandevender, TIGER: A One-Dimensional, Multilayer Electron/Photon Monte Carlo Transport Code, SLA-73-1026, Sandia Laboratories (March 1974).

21. J. A. Halbleib, Sr., and W. H. Vandevender, CYLTRAN: A Cylindrical-Geometry Multimaterial Electron/Photon Monte Carlo Transport Code, SAND 74-0030, Sandia Laboratories (March 1975).

22. G. J. Lockwood, G. H. Miller and J. A. Halbleib, Sr., Calorimetric Measurement of Electron Energy Deposition in Extended Media--Theory vs. Experiment, SAND 79-0414, Sandia Laboratories, to be published. See also IEEE Trans. Nucl. Sci. NS-20, 326 (1973); NS-21, 359 (1974); NS-22, 2537 (1975); NS-23, 1862 (1976); NS-23, 1881 (1976); and NS-25, 1581 (1978).

DISTRIBUTION:

Air Force Weapons Laboratory (4)
Kirtland Air Force Base
Albuquerque, NM 87115
Attn: L. A. Schlie, ALL
C. A. Aeby, DYC
J. F. Janni, DYC
K. Smith, DYV

University of California
Laser Gas Dynamics Laboratory
Departments of AMES
La Jolla, CA 92037
Attn: T. K. Tio

Lawrence Livermore Laboratory
University of California
P.O. Box 808
Livermore, CA 94550
Attn: F. R. Kovar

Oak Ridge National Laboratory (2)
Union Carbide Corporation
P.O. Box X
Oak Ridge, TN 37830
Attn: R. D. Birkoff
R. H. Ritchie

AVCO-Everett Research Laboratory
2385 Revere Beach Parkway
Everett, MA 02149
Attn: J. H. Jacob

Intelcom Radiation Technology
P.O. Box 80817
San Diego, CA 92138
Attn: L. Harris

Science Applications, Inc.
1651 Old Meadow Road
McLean, VA 22101
Attn: W. L. Chadsey

ARCON Corporation
18 Lakeside Office Park
Wakefield, MA 01880
Attn: S. Woolf

California Institute of Technology
Space Radiation Laboratory
Pasadena, CA 91125
Attn: C. Chen

U. S. Department of Commerce (3)
National Bureau of Standards
Washington, DC 20234
Attn: M. J. Berger
S. M. Seltzer
L. V. Spencer

RSIC, Neutron Physics Division
Oak Ridge National Laboraory
Oak Ridge, TN 37831
Attn: B. F. Maskewitz

U. S. Naval Research Laboratory (3)
Code 770
Washington, DC 20390
Attn: J. L. Block
J. B. Langworthy
S. K. Searles

Harry Diamond Laboratories (2)
2800 Powder Mill Road
Aurora Facility
Adelphi, MD
Attn: S. Graybill
K. Karas

Science Applications, Inc. (3)
1200 Prospect
La Jolla, CA 92037
Attn: A. Ciplickas
W. A. Coleman
J. Reed

Energy Sciences, Inc.
111 Terrance Hall Avenue
Burlington, MA 01803
Attn: J. Ottesin

McDonnel Douglas Astronautics Co.
5301 Bolsa Avenue
Huntington Beach, CA 92647
Attn: M. R. Westmorland

Los Alamos Scientific Laboratory (4)
P.O. Box 1663
Los Alamos, NM 87544
Attn: Report Librarian
S. Evans, T-6
C. Young, J-14
J. Mack, J-15
B. Wienke, T-1

DISTRIBUTION--cont'd

SPIRE Corporation
Patriots Park
Bedford, MA 01730
Attn: Roger Little

Maxwell Laboratories, Inc.
9244 Balboa Avenue
San Diego, CA 92123
Attn: A. Kolb

Physics International (3)
2700 Merced Street
San Leandro, CA 94577
Attn: A. J. Toepfer
S. Putnam
D. Dakin

Department of Physics
University of Texas
System Cancer Center
M. D. Anderson Hospital
and Tumor Institute
6723 Bertner
Houston, TX 77030
Attn: J. R. Marbach

U. S. Naval Research Laboratory
Code 6680
Washington, D.C. 20375
Attn: J. Criss
D. Brow

Rocketdyne
Rockwell International
3636 Menaul Blvd. N.E.
Albuquerque, NM 87110
Attn: C. Kraus

McDonnell Douglas (2)
Astronautics Company-East
St. Louis, MO 63166
Attn: R. L. Kloster
G. W. Davis

Lockheed Missiles & Spac. Co.
P.O. Box 504
Org. 6220
Sunnyvale, CA 74088
Attn: J. C. Lee

Brookhaven National Laboratory (2)
Upton, NY 11973
Attn: R. M. Sternheimer
R. F. Peierls

L'Garde, Inc.
1555 Placentia Avenue
Newport Beach, CA 92663
Attn: M. Thomas

Kaman Sciences Corp.
P.O. Box 7463
Colorado Springs, CO 80933
Attn: W. E. Ware

Fulmer Research Institute, Ltd.
STOKE POGES
SLOUGH SL2 4QD
United Kingdom
Attn: A. Holmes-Siedle

University of Toronto
Department of Chemical Engineering
and Applied Chemistry
Toronto, Canada M5S 1A4
Attn: J. S. Hewitt

Mathematical Applications Group, Inc.
180 South Broadway
White Plains, NY
Attn: W. Gruber
R. Nagle
R. Goldstein
P. S. Mittelman
M. H. Kalos

Science Applications, Inc.
P.O. Box 2351
1250 Prospect Street
La Jolla, CA 92037
Attn: E. A. Straker
W. H. Scott, Jr.
N. R. Byrn

Mission Research Corp.
735 State Street
Santa Barbara, CA 93101
Attn: C. L. Longmire

Peter Almond
Physics Department
M. D. Anderson Hospital
Texas Medical Center
Houston, TX 77030

Anders Brahme
Dept. of Radiation Physics
Karolinska Institute
Fack
S-104 01 Stockholm, Sweden

Andree Dutreix
Institut Gustave Roussy
94 800 Villejuif, France

Dietrich Harder
Institut fur Medizinische Physik
und Biophysik
D 3400 Gottingen
Gosslerstr. 10, West Germany

Mr. & Mrs. Hans Leetz
Institut t. Biophysik
Univ. Kliniken
D-6650 Homberg 3, West Germany

Hans Svensson
Radiation Physics Department
Regional Hospital
S-901 85 Umea, Sweden

Andre Wambersie
Unite de Radiotherapie et de
Neutrontherapie
Centre des Tumerus UCL 54.69
av. Hippocrate, 54
B. 1200 Bruxelles, Belgium

Air Force Cambridge Research Lab (4)
L. G. Hanscom Field
Beford, MA 01730
Attn: J. N. Bradford
E. A. Burke
A. R. Frederickson
J. C. Garth

Northrup Research
& Technology Center (2)
3401 W. Broadway
Hawthorne, CA 90250
Attn: W. Hant
G. Duckworth

The Aerospace Corporation (4)
P.O. Box 92957
Los Angeles, CA 90009
Attn: D. G. Swanson
C. Crummer
R. Pruett
C. Greenhow

Experimental & Mathematical
Physics Consultants
Box 66331
Los Angeles, CA 90066
Attn: T. M. Jordan

Northrup Corporation
Electronics Division
A3144/A60
2301 W. 120th Street
Hawthorne, CA 90250
Attn: L. T. Smith

1100 C. D. Broyles
1110 J. D. Kennedy
1111 C. R. Mehl
1111 F. F. Dean
1112 K. M. Glibert
1112 J. Harris
1112 J. J. Hohlfelder
1112 D. R. Waymire
1115 T. J. Flanagan
1116 J. D. Plimpton
2116 W. J. Barnard
2116 D. H. Habing
2140 B. L. Gregory
2141 D. L. Weaver
2151 R. C. Heckman
2155 G. W. Krause
2165 J. E. Gover
2331 H. L. Floyd, Jr.
2355 R. W. Barnard
2355 D. H. Jensen
2531 T. J. Young
2531 D. R. Koehler
2623 W. H. Vandevender
3312 T. N. Simmons
4000 A. Narath
Attn: 4300 R. L. Peurifoy
4400 A. W. Snyder
4500 E. H. Beckner
4700 J. H. Scott
4200 G. Yonas
4210 J. B. Gerardo
4211 E. J. McGuire

DISTRIBUTION--cont'd

4211 M. K. Matzen
4211 M. E. Riley
4212 R. A. Gerber
4212 G. N. Hays
4212 J. M. Hoffman
4212 E. L. Patterson
4212 J. K. Rice
4216 G. H. Miller
4216 A. W. Johnson
4230 M. Cowan
4231 J. H. Renken
4231 F. Biggs
4231 S. A. Dupree
4231 T. A. Green
4231 J. A. Halbleib, Sr. (25)
4231 C. J. MacCallum
4231 P. J. McDaniel
4231 J. E. Morel
4231 J. M. Peek
4231 C. N. Vittitoe
4232 W. Beezhold
4232 P. E. Bolduc
4232 W. H. Buckalew
4232 L. W. Kruse
4232 C. R. McClenahan
4232 H. N. Woodall
4234 R. E. Palmer
4240 G. W. Kuswa
4241 J. R. Freeman
4241 T. P. Wright
4242 L. P. Mix
4242 E. J. Burns
4242 J. Chang
4242 R. J. Leeper
4242 F. C. Perry
4244 P. A. Miller
4244 J. N. Olsen
4247 M. M. Widner
4247 M. J. Clauser
4247 A. V. Farnsworth
4247 M. A. Sweeney
4250 T. H. Martin
4252 J. P. Vandevender
4252 D. L. Johnson
4253 K. R. Prestwich
4253 M. T. Buttram
4253 R. B. Miller
4253 J. J. Ramirez
4254 S. A. Goldstein
4330 E. E. Ives

4340 H. W. Schmitt
4343 J. L. Duncan
4343 F. N. Coppage
4343 E. F. Hartman
4360 J. A. Hood
4411 L. L. Bonzon
4411 L. D. Buxton
4420 J. V. Walker
4423 J. E. Powell
4423 D. A. McArthur
4424 J. Odom
4514 F. W. Bingham
4536 C. M. Percival
5521 O. L. Burchett
5531 L. D. Bertholf
5532 B. M. Bucher
5535 J. Lipkin
5534 D. A. Benson
5536 A. J. Chabai
5811 L. A. Harrah
5815 T. S. Prevender
8266 (1)E. A. Ass
8341 L. G. Haggmark

3141 (5) T. L. Werner
3151 (3) W. L. Garner for DOE/TIC
3154-3 (25) for DOE/TIC

Argonne National Laboratory
9700 S. Cass Avenue
Argonne IL 60436
Attn: Argonne Code Center